

# Supplementary Material

The following tables report parameters and compare vibrational band origins as discussed in the paper **Algebraic-matrix calculation of vibrational levels of triatomic molecules** by T. Šedivcová-Uhlíková, Hewa Y. Abdullah, and Nicola Manini.

TABLE A. Fitting parameters (in Hartree atomic units) for the  $R_i^{-p}$  expansions in Morse coordinates, Eq. (11) of the main text, for the studied molecules. The fits are carried out in the following ranges:  $R_{OC} = 1.32 \div 4.7$  a.u.,  $R_{CS} = 2.4 \div 3.78$  a.u.,  $R_{HC} = 1.5 \div 3.5$  a.u.,  $R_{CN} = 1.6 \div 3.0$  a.u.,  $R_{NO} = 1.9 \div 3.2$  a.u.,  $R_{OH} = 1.35 \div 3.2$  a.u.

system	$b_0$	$b_1$	$b_2$	$b_3$	$b_4$	$b_5$
$R_{OC}^{-1}$	0.457685	0.169226	-0.021905	0.015526	-0.013160	0.015850
$R_{OC}^{-2}$	0.209479	0.154873	0.008480	0.007549	-0.004657	0.005804
$R_{CS}^{-1}$	0.338904	0.111322	-0.018657	0.012254	-0.011645	0.008461
$R_{CS}^{-2}$	0.114859	0.075453	-0.000423	0.004164	-0.003489	0.002530
$R_{HC}^{-1}$	0.496627	0.254217	0.003579	0.013680	-0.015465	0.026987
$R_{HC}^{-2}$	0.246653	0.252068	0.067223	0.020238	-0.000780	0.008569
$R_{CN}^{-1}$	0.458835	0.171067	-0.020751	0.019016	-0.016428	0.007374
$R_{CN}^{-2}$	0.210545	0.157132	0.009775	0.008909	-0.005792	0.002694
$R_{ON}^{-1}$	0.445632	0.118759	-0.025096	0.007967	-0.021604	0.026137
$R_{ON}^{-2}$	0.198628	0.105467	-0.009673	0.004369	-0.009938	0.011674
$R_{HO}^{-1}$	0.551962	0.261286	-0.003594	0.003427	-0.027048	0.041423
$R_{HO}^{-2}$	0.304789	0.286850	0.059773	0.013633	-0.007170	0.014774

TABLE B. The values of potential-energy parameters for HCN ( $R_1 = 2.0135$  a.u.,  $\alpha_1 = 0.9727$  a.u. $^{-1}$  for CH, and  $R_2 = 2.1793$  a.u.,  $\alpha_2 = 1.2290$  a.u. $^{-1}$  for CN), in Hartree atomic units. The form of the potential energy function is given by Eq. (3) in the main text.

$k_1$	$k_2$	$k_3$	$a_{k_1 k_2 k_3}$	$k_1$	$k_2$	$k_3$	$a_{k_1 k_2 k_3}$	$k_1$	$k_2$	$k_3$	$a_{k_1 k_2 k_3}$
0	0	1	0.059318	1	1	0	-0.010473	3	0	1	0.008907
0	0	2	0.011186	1	2	0	0.007719	0	1	1	0.060746
0	0	3	0.008006	1	3	0	-0.002693	0	1	2	0.003288
0	0	4	-0.008333	2	1	0	0.004400	0	1	3	-0.015908
1	0	0	-0.000455	2	2	0	-0.010019	0	2	1	-0.028872
2	0	0	0.211513	3	1	0	-0.005224	0	2	2	0.005894
3	0	0	0.009211	1	0	1	0.016978	0	3	1	0.037804
4	0	0	0.030108	1	0	2	0.019794	1	1	1	0.022503
0	1	0	-0.000791	0	3	1	0.002993	1	1	2	-0.018163
0	2	0	0.397690	2	0	1	-0.013440	1	2	1	-0.007818
0	3	0	-0.022029	2	0	2	0.007265	2	1	1	-0.021432
0	4	0	0.018340								

TABLE Ca. Comparison between observed and computed purely vibrational  $m = 0$  band origins [ $\text{cm}^{-1}$ ] of OCS.

$(v_1 v_2 v_3)$	$E_v^{\text{obs}}$	$E_v^{\text{cal}}$	$E_v^{\text{obs}} - E_v^{\text{cal}}$
(1 0 0)	858.97	858.94	0.03
(0 2 0)	1047.04	1047.05	-0.01
(2 0 0)	1710.98	1710.85	0.13
(1 2 0)	1892.23	1892.41	-0.18
(0 0 1)	2062.20	2061.98	0.22
(0 4 0)	2104.83	2104.69	0.14
(3 0 0)	2555.99	2555.73	0.26
(2 2 0)	2731.40	2731.65	-0.25
(1 0 1)	2918.11	2917.90	0.21
(1 4 0)	2937.15	2937.17	-0.02
(0 2 1)	3095.55	3095.27	0.28
(0 6 0)	3170.64	3170.38	0.26
(4 0 0)	3393.97	3393.57	0.40
(3 2 0)	3564.48	3564.73	-0.25
(2 4 0)	3762.83	3762.90	-0.07
(2 0 1)	3768.50	3768.26	0.24
(1 2 1)	3937.43	3937.42	0.01
(1 6 0)	3990.11	3989.93	0.18
(0 0 2)	4101.39	4101.20	0.19
(0 4 1)	4141.21	4140.86	0.35
(5 0 0)	4224.87	4224.38	0.50
(0 8 0)	4242.55	4242.26	0.29
(4 2 0)	4391.41	4391.63	-0.22
(3 4 0)	4585.25	4585.38	-0.13
(3 0 1)	4609.85	4609.45	0.40
(2 2 1)	4773.22	4773.36	-0.14
(2 6 0)	4805.16	4805.03	0.13
(1 0 2)	4953.88	4953.75	0.13
(1 4 1)	4970.43	4970.36	0.07
(6 0 0)	5048.62	5048.13	0.49
(1 8 0)	5049.14	5048.83	0.31
(0 2 2)	5120.98	5120.64	0.34
(0 6 1)	5196.01	5195.72	0.29
(5 2 0)	5212.14	5212.31	-0.17
(0 10 0)	5319.02	5318.84	0.18
(4 4 0)	5401.48	5401.58	-0.10
(4 0 1)	5444.96	5444.45	0.51
(3 2 1)	5602.47	5602.64	-0.17
(3 6 0)	5616.07	5615.95	0.12
(2 4 1)	5792.00	5792.15	-0.15
(2 0 2)	5801.91	5801.68	0.22
(2 8 0)	5852.00	5851.66	0.34
(7 0 0)	5865.18	5864.82	0.36
(1 2 2)	5959.33	5959.37	-0.04
(1 6 1)	6012.06	6011.95	0.11
(6 2 0)	6026.59	6026.74	-0.15
(1 10 0)	6112.59	6112.28	0.31
(0 0 3)	6117.58	6117.64	-0.06
(0 4 2)	6154.70	6154.36	0.34
(5 4 0)	6212.12	6212.16	-0.04
(0 8 1)	6257.83	6257.74	0.09
(5 0 1)	6273.13	6272.51	0.62
(0 12 0)	6398.77	6398.83	-0.06

TABLE Ca. Continued

$(v_1 v_2 v_3)$	$E_v^{\text{obs}}$	$E_v^{\text{cal}}$	$E_v^{\text{obs}} - E_v^{\text{cal}}$
(460)	6418.68	6418.46	0.22
(421)	6429.10	6429.31	-0.21
(341)	6611.11	6611.31	-0.20
(302)	6640.10	6639.80	0.30
(380)	6650.90	6650.55	0.35
(800)	6674.46	6674.41	0.04
(222)	6791.54	6791.81	-0.27
(261)	6823.87	6823.86	0.01
(720)	6834.69	6834.89	-0.20
(2100)	6903.16	6902.78	0.38
(103)	6966.17	6966.32	-0.15
(142)	6980.96	6981.00	-0.04
(640)	7017.13	7017.11	0.02
(181)	7060.66	7060.59	0.07
(601)	7094.22	7093.59	0.63
(023)	7123.38	7123.16	0.22
(1120)	7179.14	7179.02	0.12
(062)	7198.75	7198.61	0.14
(560)	7220.13	7219.81	0.32
(521)	7245.75	7246.00	-0.25
(0101)	7324.96	7325.20	-0.24
(441)	7423.79	7423.92	-0.13
(480)	7445.74	7445.45	0.29
(402)	7472.18	7471.77	0.41
(900)	7476.38	7476.94	-0.56
(0140)	7480.69	7481.16	-0.47
(322)	7616.85	7617.19	-0.34
(361)	7631.94	7632.02	-0.08
(820)	7636.35	7636.71	-0.36
(3100)	7690.33	7689.95	0.38
(242)	7797.96	7798.39	-0.42
(203)	7811.95	7811.94	0.01
(740)	7816.43	7816.39	0.04
(281)	7859.95	7859.91	0.04
(701)	7908.22	7907.66	0.56
(2120)	7957.27	7957.12	0.15
(123)	7958.04	7958.28	-0.24
(162)	8011.27	8011.42	-0.15
(660)	8015.70	8015.31	0.39
(621)	8057.05	8057.29	-0.24

TABLE Cb. Comparison between observed and computed  $m = 1$  vibrational band origins [ $\text{cm}^{-1}$ ] of OCS.

$(v_1 v_2 v_3)$	$E_v^{\text{obs}}$	$E_v^{\text{cal}}$	$E_v^{\text{obs}} - E_v^{\text{cal}}$
(010)	520.42	520.70	-0.27
(110)	1372.46	1372.85	-0.39
(030)	1573.37	1573.52	-0.16
(210)	2218.03	2218.45	-0.42
(130)	2412.12	2412.47	-0.35
(011)	2575.31	2575.30	0.01
(050)	2635.59	2635.59	0.00
(310)	3057.09	3057.48	-0.39
(230)	3245.26	3245.70	-0.44
(111)	3424.14	3424.33	-0.19
(150)	3461.58	3461.71	-0.13
(031)	3615.34	3615.23	0.11
(070)	3704.77	3704.68	0.09
(410)	3889.61	3889.93	-0.32
(330)	4072.69	4073.15	-0.46
(211)	4266.32	4266.61	-0.29
(250)	4282.91	4283.09	-0.18
(131)	4450.76	4450.96	-0.20
(170)	4517.94	4517.88	0.06
(012)	4607.11	4607.06	0.05
(051)	4666.09	4665.96	0.14
(510)	4715.54	4715.79	-0.26
(090)	4779.23	4779.16	0.07
(430)	4894.35	4894.77	-0.42
(350)	5097.05	5097.26	-0.22
(311)	5104.23	5104.50	-0.27
(231)	5280.54	5280.93	-0.39
(270)	5327.03	5326.96	0.07
(112)	5452.46	5452.68	-0.22
(151)	5488.78	5488.90	-0.12
(610)	5534.81	5535.04	-0.24
(190)	5579.46	5579.32	0.15
(032)	5634.23	5634.08	0.16
(530)	5710.14	5710.51	-0.37
(071)	5724.78	5724.76	0.02
(0110)	5857.57	5857.68	-0.11
(450)	5908.98	5909.11	-0.14
(411)	5932.73	5933.00	-0.27
(331)	6104.52	6104.97	-0.45
(370)	6131.88	6131.81	0.07
(212)	6290.91	6291.31	-0.40
(251)	6307.12	6307.37	-0.25
(710)	6347.35	6347.66	-0.31
(290)	6376.32	6376.15	0.17
(132)	6466.15	6466.44	-0.29
(630)	6520.02	6520.33	-0.32
(171)	6534.40	6534.51	-0.11
(013)	6615.85	6615.96	-0.10
(1110)	6644.69	6644.72	-0.02
(052)	6673.76	6673.71	0.06
(550)	6714.77	6714.83	-0.06
(511)	6755.61	6755.84	-0.23
(091)	6789.57	6789.84	-0.27
(431)	6921.91	6922.20	-0.29
(390)	6933.04	6933.14	-0.10
(0130)	6938.60	6939.16	-0.55
(351)	7116.51	7116.93	-0.42
(312)	7126.90	7127.26	-0.37

TABLE Cb. Continued

$(v_1 v_2 v_3)$	$E_v^{\text{obs}}$	$E_v^{\text{cal}}$	$E_v^{\text{obs}} - E_v^{\text{cal}}$
(810)	7153.07	7153.60	-0.52
(470)	7169.47	7169.43	0.04
(232)	7292.42	7293.00	-0.58
(730)	7323.89	7324.20	-0.31
(271)	7340.06	7340.35	-0.28
(2110)	7429.19	7429.58	-0.39
(113)	7457.43	7457.87	-0.44
(152)	7493.10	7493.44	-0.34
(650)	7515.15	7515.15	0.01
(611)	7572.02	7572.22	-0.20
(191)	7585.81	7586.33	-0.53
(033)	7630.11	7630.10	0.01
(1130)	7712.37	7713.60	-1.23
(072)	7722.39	7722.74	-0.35
(570)	7725.25	7725.09	0.16
(531)	7737.80	7738.39	-0.59
(0111)	7858.90	7860.06	-1.17
(451)	7925.38	7925.82	-0.44
(412)	7951.73	7952.04	-0.32
(910)	7951.89	7952.94	-1.05
(490)	7958.81	7959.27	-0.47

TABLE D. The observed vibrational band origins [ $\text{cm}^{-1}$ ] of HCN are compared to those computed using the present approach and to those computed in the Reference work by van Mourik *et al.* [26]. A few predicted levels are also listed.

$(v_1 v_2 v_3)$	$E_v^{\text{obs}}$	$E_v^{\text{cal}}$	$E_v^{\text{obs}} - E_v^{\text{cal}}$	$E_v^{\text{Ref}}$	$E_v^{\text{obs}} - E_v^{\text{Ref}}$
(020)	1411.42	1412.4	-1.0	1414.9	-3.5
(001)	2096.85	2101.7	-4.9	2100.5	-3.7
(040)	2802.96	2807.8	-4.8	2801.4	1.7
(100)	3311.48	3314.2	-2.7	3307.7	3.8
(021)	3502.12	3508.3	-6.2	3510.9	-8.8
(060)	4174.61	4183.3	-8.7	4176.2	-1.6
(002)	4173.07	4185.9	-12.8	4181.4	-8.3
(120)	4684.31	4686.9	-2.6	4686.2	-1.9
(041)	4888.00	4897.8	-9.8	4891.7	-3.7
(101)	5393.70	5401.5	-7.8	5394.4	-0.7
(080)	5525.81	5545.6	-19.8	5537.7	-11.9
(022)	5571.89	5583.5	-11.6	5586.5	-14.6
(140)	6036.96	6042.6	-5.6	6033.7	3.3
(003)	6228.60	6244.7	-16.1	6242.4	-13.8
(061)	6254.38	6270.1	-15.7	6260.5	-6.1
(200)	6519.61	6529.1	-9.5	6513.5	6.1
(121)	6761.33	6768.7	-7.4	6768.5	-7.2
(0100)	6855.53	6884.7	-29.2	6879.6	-24.1
(042)	6951.68	6966.7	-15.0	6960.9	-9.2
(160)	-	7381.1	-	7369.1	-
(102)	7455.42	7468.8	-13.4	7461.6	-6.2
(081)	-	7623.8	-	7617.2	-
(023)	-	7638.0	-	7641.2	-
(220)	7853.51	7861.7	-8.2	7855.8	-2.3
(141)	8107.97	8118.8	-10.8	8110.2	-2.2
(0120)	-	8200.8	-	8197.5	-
(004)	-	8286.0	-	8283.3	-
(062)	-	8332.6	-	8323.5	-
(201)	8585.58	8600.4	-14.8	8584.7	0.9
(180)	-	8701.3	-	8691.6	-
(122)	8816.00	8829.9	-13.9	8830.2	-14.2
(0101)	-	8957.0	-	8954.4	-
(043)	8995.22	9014.4	-19.18	9009.0	-13.8
(240)	-	9177.4	-	9164.0	-
(161)	-	9451.8	-	9440.1	-
(0140)	-	9490.7	-	9488.5	-
(103)	9496.44	9516.0	-19.6	9508.9	-12.5
(300)	9627.09	9645.4	-18.3	9619.2	7.9
(024)	-	9671.7	-	9674.6	-
(082)	-	9680.0	-	9675.2	-
(221)	9914.4	9928.2	-13.8	9922.9	-8.5
(1100)	-	10001.0	-	9993.9	-
(142)	-	10173.7	-	10165.6	-
(0121)	-	10267.0	-	10266.4	-
(005)	-	10306.9	-	10304.1	-
(063)	-	10373.5	-	10364.9	-
(260)	-	10476.1	-	10460.5	-
(202)	10631.4	10652.2	-20.8	10636.7	-5.3
(0160)	-	10751.0	-	10749.7	-
(181)	-	10766.2	-	10758.0	-
(123)	-	10870.0	-	10871.1	-
(320)	-	10937.3	-	10925.3	-
(0102)	10974.2	11006.9	-32.7	11006.5	-32.3

TABLE D. Continued

$(v_1 v_2 v_3)$	$E_v^{\text{obs}}$	$E_v^{\text{cal}}$	$E_v^{\text{obs}} - E_v^{\text{cal}}$	$E_v^{\text{Ref}}$	$E_v^{\text{obs}} - E_v^{\text{Ref}}$
(044)	11015.9	11040.8	-24.9	11035.7	-19.8
(241)	-	11239.0	-	11225.9	-
(1120)	-	11277.5	-	11271.7	-
(162)	-	11500.5	-	11489.4	-
(0141)	-	11542.9	-	11536.1	-
(104)	11516.6	11550.9	-34.3	11549.6	-33.0
(301)	11674.5	11684.5	-10	11672.8	1.7
(025)	-	11698.5	-	11688.1	-
(083)	-	11714.2	-	11710.1	-
(280)	-	11756.7	-	11744.5	-
(222)	-	11974.5	-	11969.9	-
(0180)	-	11978.0	-	11977.7	-
(1101)	-	12060.1	-	12055.7	-
(143)	-	12206.2	-	12192.5	-
(340)	-	12213.4	-	12200.6	-
(006)	-	12307.5	-	12304.5	-
(0122)	-	12310.6	-	12311.7	-
(064)	-	12392.9	-	12382.0	-

TABLE E. Comparison between observed and computed vibrational band origins [ $\text{cm}^{-1}$ ] of  $\text{NO}_2$ .

$(v_1 v_2 v_3)$	$E_v^{\text{obs}}$	$E_v^{\text{cal}}$	$E_v^{\text{obs}} - E_v^{\text{cal}}$
(010)	749.649	749.48	0.17
(100)	1319.794	1320.67	-0.88
(020)	1498.34	1498.22	0.12
(001)	1616.852	1618.34	-1.49
(110)	2063.118	2062.35	0.78
(030)	2246.04	2245.90	0.14
(011)	2355.151	2355.65	-0.50
(200)	2627.337	2629.17	-1.83
(120)	2805.6	2804.41	1.19
(101)	2906.074	2905.53	0.54
(040)	2993.0	2992.36	0.64
(021)	3092.481	3092.90	-0.42
(002)	3201.433	3202.20	-0.77
(210)	3364.57	3364.02	0.55
(130)	3547.1	3545.96	1.14
(111)	3637.843	3635.84	2.00
(050)	3738.6	3737.55	1.05
(031)	3829.34	3829.52	-0.18
(300)	3922.61	3923.95	-1.34
(012)	3929.12	3928.97	0.15
(220)	4100.58	4099.75	0.83
(201)	4179.938	4177.90	2.04
(140)	4286.82	4286.42	0.40
(121)	4369.1	4366.68	2.42
(102)	4461.07	4458.63	2.44
(060)	4482.57	4481.44	1.13
(041)	4564.22	4565.11	-0.89
(310)	4652.0	4651.01	0.99
(022)	4656.34	4656.38	-0.04
(003)	4754.209	4753.80	0.41
(230)	4835.05	4835.05	0.00
(211)	4905.52	4901.97	3.55
(150)	5025.2	5025.31	-0.11
(131)	5098.0	5097.07	0.93
(112)	5180.54	5177.47	3.07
(400)	5205.81	5207.49	-1.68
(070)	5224.55	5224.03	0.52
(051)	5298.16	5299.39	-1.23
(032)	5377.91	5377.30	0.61
(320)	5384.41	5384.69	-0.28
(301)	5437.54	5434.25	3.29
(013)	5469.66	5468.64	1.02
(240)	5568.41	5568.93	-0.52
(221)	5630.36	5626.62	3.74
(202)	5701.41	5698.37	3.04
(160)	5762.23	5762.25	-0.02
(141)	5826.29	5826.29	0.00
(122)	5898.94	5896.50	2.44
(410)	5930.66	5930.69	-0.03
(080)	5965.61	5965.30	0.31
(103)	5984.705	5981.83	2.88



TABLE E. Continued

$(v_1 v_2 v_3)$	$E_v^{\text{obs}}$	$E_v^{\text{cal}}$	$E_v^{\text{obs}} - E_v^{\text{cal}}$
(061)	6030.71	6032.06	-1.35
(042)	6101.80	6101.79	0.01
(330)	6112.11	6112.77	-0.66
(311)	6156.25	6152.20	4.05
(023)	6183.61	6182.94	0.67
(004)	6275.98	6274.83	1.15
(250)	6299.70	6300.57	-0.87
(231)	6351.40	6350.62	0.78
(212)	6414.16	6411.21	2.95
(500)	6475.05	6475.27	-0.22
(170)	6497.60	6496.88	0.72
(151)	6552.84	6553.69	-0.85
(132)	6616.53	6614.85	1.68
(420)	6653.54	6654.00	-0.46
(401)	6676.86	6672.05	4.81
(113)	6693.12	6692.31	0.81
(090)	6705.23	6705.18	0.05
(071)	6771.44	6762.82	8.62
(052)	6823.80	6824.39	-0.59
(340)	6837.75	6838.95	-1.2
(321)	6872.10	6870.35	1.75
(033)	6897.37	6896.11	1.26
(302)	6921.67	6920.44	1.23
(014)	6979.21	6977.98	1.23
(260)	7029.48	7029.18	0.30
(241)	7072.23	7072.92	-0.69
(222)	7125.60	7123.90	1.70
(203)	7192.29	7191.82	0.47
(510)	7193.35	7192.88	0.47
(180)	7231.06	7228.80	2.26
(161)	7277.83	7278.63	-0.80
(142)	7332.45	7331.72	0.73
(430)	7374.57	7375.49	-0.92
(411)	7386.33	7382.08	4.25
(123)	7403.04	7402.08	0.96
(0100)	7443.09	7443.40	-0.31
(104)	7478.02	7476.38	1.64
(081)	7492.23	7491.24	0.99
(062)	7544.62	7544.93	-0.31
(350)	7562.47	7561.88	0.59
(331)	7587.04	7587.25	-0.21
(043)	7609.57	7607.70	1.87
(312)	7627.14	7627.15	-0.01
(024)	7681.49	7679.79	1.70
(600)	7730.08	7727.56	2.52
(270)	7757.29	7753.98	3.31
(005)	7766.28	7766.57	-0.29
(251)	7791.18	7792.56	-1.38
(232)	7834.97	7835.43	-0.46
(213)	7888.16	7884.58	3.58
(520)	7909.46	7905.79	3.67
(501)	7903.54	7909.62	-6.08
(190)	7962.27	7957.47	4.80

TABLE E. Continued

$(v_1 v_2 v_3)$	$E_v^{\text{obs}}$	$E_v^{\text{cal}}$	$E_v^{\text{obs}} - E_v^{\text{cal}}$
(171)	8000.93	8000.40	0.53
(152)	8046.44	8046.39	0.05
(440)	8093.61	8091.13	2.48
(421)	8093.10	8093.50	-0.4
(133)	8110.13	8110.59	-0.46
(402)	8120.70	8123.66	-2.96
(114)	8174.27	8173.90	0.37
(0110)	8178.27	8179.34	-1.07
(091)	8218.84	8216.63	2.21
(072)	8264.28	8263.22	1.06
(360)	8284.17	8280.23	3.94
(341)	8299.45	8301.69	-2.24
(053)	8320.00	8317.42	2.58
(322)	8330.35	8333.20	-2.85
(303)	8374.58	8379.91	-5.33
(034)	8382.64	8382.98	-0.34
(610)	8441.44	8439.54	1.90
(015)	8457.15	8457.35	-0.20
(280)	8482.12	8473.96	8.16
(261)	8507.33	8508.48	-1.15
(242)	8542.25	8544.87	-2.62
(223)	8585.54	8584.47	1.07
(511)	8608.92	8613.47	-4.55
(530)	8623.34	8623.21	0.13
(204)	8652.27	8658.91	-6.64
(1100)	8690.72	8682.00	8.72
(181)	8721.11	8718.07	3.04
(162)	8758.28	8758.18	0.10
(431)	8797.95	8797.80	0.15
(450)	8809.81	8806.33	3.48
(412)	8817.61	8817.08	0.53
(143)	8816.65	8823.37	-6.72
(124)	8868.35	8869.19	-0.84
(0120)	8911.29	8911.52	-0.23
(105)	8941.28	8937.70	3.58
(0101)	8944.50	8943.12	1.38
(700)	8968.55	8962.76	5.79
(082)	8982.08	8979.28	2.80

TABLE Fa The observed vibrational band origins [ $\text{cm}^{-1}$ ] of A symmetry of  $\text{H}_2\text{O}$  are compared to those computed using the present method and to those computed in the Reference work by Lemus *et al.* [23]. A few predicted levels are also listed.

$(v_1 v_2 v_3)$	$E_v^{\text{obs}}$	$E_v^{\text{cal}}$	$E_v^{\text{obs}} - E_v^{\text{cal}}$	$E_v^{\text{Ref}}$	$E_v^{\text{obs}} - E_v^{\text{Ref}}$
(010)	1594.75	1594.6	0.2	1591.55	3.2
(020)	3151.63	3151.7	-0.1	3152.42	-0.8
(100)	3657.05	3656.6	0.5	3658.13	-1.1
(030)	4666.8	4667.3	-0.5	4669.52	-2.7
(110)	5235.0	5235.4	-0.4	5234.45	0.6
(040)	6134.03	6136.2	-2.2	6133.06	1.0
(120)	6775.1	6776.3	-1.2	6780.47	-5.4
(200)	7201.54	7201.7	-0.2	7200.73	0.8
(002)	7445.07	7445.8	-0.7	7449.74	-4.7
(050)	7542.39	7549.5	-7.1	7535.94	6.5
(130)	8273.98	8275.6	-1.6	8278.81	-4.8
(210)	8761.59	8763.0	-1.4	8760.7	0.9
(060)	8890.5	8891.5	-1.0	8872.85	17.7
(012)	9000.14	9000.9	-0.8	8996.45	3.7
(140)	-	9726.4	-	9721.96	-
(070)	-	10134.8	-	10140.2	-
(220)	10284.4	10286.7	-2.3	10289.1	-4.7
(022)	10524.3	10523.1	1.2	10523.7	0.6
(300)	10599.7	10603.4	-3.7	10597.9	1.8
(102)	10868.9	10868.1	0.8	10870.8	-1.9
(310)	12139.2	12144.5	-5.3	12136.0	3.2
(112)	12407.6	12408.7	-1.1	12404.5	3.1
(240)	13205.1	13205.5	-0.4	13193.9	11.2
(042)	13448.0	13455.8	-7.8	13457.0	-9.0
(122)	13642.2	13648.0	-5.8	13643.4	-1.2
(202)	13828.3	13818.5	9.8	13826.9	1.4
(122)	13910.9	13913.8	-2.9	13914.5	-3.6
(400)	14221.2	14219.0	2.2	14221.7	-0.5
(004)	14536.5	14539.5	-3.0	14532.5	4.0
(132)	15107.0	15106.4	0.6	15104.9	2.1
(212)	15344.5	15355.7	-11.2	15341.6	2.9
(410)	15742.8	15743.8	-1.0	15740.4	2.4
(222)	16825.2	16836.0	-10.8	16824.6	0.6
(302)	16898.4	16914.4	-16.0	16898.7	-0.3
(420)	17227.7	17229.8	-2.1	17231.2	-3.5
(500)	17458.3	17458.7	-0.4	17455.8	2.5
(104)	17748.1	17747.1	1.0	17746.5	1.6

TABLE Fb The observed vibrational band origins [ $\text{cm}^{-1}$ ] of B symmetry of  $\text{H}_2\text{O}$  are compared to those computed using the present method and to those computed in the Reference work by Lemus *et al.* [LEMUS - final reference !!!].

$(v_1 v_2 v_3)$	$E_v^{\text{obs}}$	$E_v^{\text{cal}}$	$E_v^{\text{obs}} - E_v^{\text{cal}}$	$E_v^{\text{Ref}}$	$E_v^{\text{obs}} - E_v^{\text{Ref}}$
(001)	3755.93	3757.0	-1.1	3762.48	-6.6
(011)	5331.27	5331.8	-0.5	5329.2	2.1
(021)	6871.51	6872.1	-0.6	6873.16	-1.7
(101)	7249.81	7252.0	-2.2	7253.5	-3.7
(031)	8373.85	8374.6	-0.8	8377.65	-3.8
(111)	8807.0	8809.6	-2.6	8804.8	2.2
(041)	9833.58	9835.0	-1.4	9832.29	1.3
(121)	10328.7	10331.7	-3.0	10331.3	-2.6
(201)	10613.4	10618.1	-4.7	10615.4	-2.0
(003)	11032.4	11034.0	-1.6	11032.8	-0.4
(051)	-	11246.6	-	11229.4	-
(131)	11813.2	11816.0	-2.8	11815.2	-2.0
(211)	12151.3	12157.1	-5.8	12149.2	2.1
(013)	12565.0	12567.3	-2.3	12557.1	7.9
(061)	-	12598.1	-	12563.1	-
(141)	13256.2	13258.0	-1.8	13248.9	7.3
(221)	13652.7	13659.1	-6.4	13655.7	-3.0
(071)	13835.4	13837.7	-2.3	13829.5	5.9
(023)	14066.2	14069.9	-3.7	14066.8	-0.6
(103)	14318.8	14320.8	-2.0	14319.7	-0.9
(151)	14640.0	14648.4	-8.4	14626.2	13.8
(231)	15119.0	15125.0	-6.0	15118.9	0.1
(311)	15348.0	15359.7	-11.7	15345.9	2.1
(033)	15534.7	15539.6	-4.9	15543.9	-9.2
(113)	15832.8	15837.5	-4.7	15825.2	7.6
(321)	16821.6	16834.6	-13.0	16824.4	-2.8
(203)	16898.8	16914.7	-15.9	16899.2	-0.4
(123)	17312.5	17319.5	-7.0	17314.3	-1.8
(401)	17495.5	17498.8	-3.3	17500.	-4.5

# Algebraic-matrix calculation of vibrational levels of triatomic molecules

T. Šedivcová-Uhlíková<sup>1,\*</sup>, Hewa Y. Abdullah<sup>1,2</sup>, and Nicola Manini<sup>1</sup>

<sup>1</sup>*Physics Department and INFN - University of Milan  
and European Theoretical Spectroscopy Facility  
Via Celoria 16, 20133 Milano, Italy*

<sup>2</sup>*Physics Department, College of Science Education  
Salahaddin University, Erbil, Iraq*

(Dated: December 1, 2008)

We introduce an accurate and efficient algebraic technique for the computation of the vibrational spectra of triatomic molecules, of both linear and bent equilibrium geometry. The full three-dimensional potential energy surface (PES), which can be based on entirely *ab initio* data, is parameterized as a product Morse-cosine expansion, expressed in bond-angle internal coordinates, and includes explicit interactions among the local modes. We describe the stretching degrees of freedom in the framework of a Morse-type expansion on a suitable algebraic basis, which provides exact analytical expressions for the elements of a sparse Hamiltonian matrix. Likewise, we use a cosine power expansion on a spherical harmonics basis for the bending degree of freedom. The resulting matrix representation in the product space is very sparse and vibrational levels and eigenfunctions can be obtained by efficient diagonalization techniques. We apply this method to carbonyl sulfide OCS, hydrogen cyanide HCN, water H<sub>2</sub>O, and nitrogen dioxide NO<sub>2</sub>. When we base our calculations on high-quality PESs tuned to the experimental data, the computed spectra are in very good agreement with the observed band origins.

PACS numbers: 33.20.Tp, 31.15.-p, 31.50.Bc, 03.65.Fd, 33.15.Mt

Keywords: vibrational states, three atomic molecules, algebraic methods

## I. INTRODUCTION

The present-day fast development of new spectroscopic instruments and methods allows us to measure vibrational states with high accuracy even in the energy region near the molecular dissociation [1, 2, 3]. Characterizing these new experimental data is especially important for instance, for understanding the dynamics of chemical reactions and for analyzing spectra from remote regions (e.g., upper atmosphere and/or interstellar matter), where strong radiation along with low pressure can stabilize molecules in extraordinarily excited states, sometimes promoting unusual reactions. All energy levels depend sensitively on the detailed shape of the molecular potential energy surface (PES). Their qualitative and also quantitative description calls for the development of more and more accurate theoretical approaches [3, 4, 5, 6, 7, 8].

Present-day status of the art program codes for the accurate calculation of vibrational spectra of small molecules have been developed in J. Tennyson's (TRIATOM [4], DVR3R [5] ...) and P. Jensen's (MORBID [6], TROVE [7]) groups. They are based on different approaches and find best use for different kinds of small (in particular triatomic) molecules. TRIATOM focuses mainly on van der Waals complexes, and employs Legendre and Laguerre polynomials as basis functions. The matrix elements are integrated numerically using a discrete variable representation (DVR) based on Gauss-Jacobi and Gauss-Laguerre quadrature for all 3 internal coordinates. The resulting spectra depend on the DVR grid in a non-variational fashion. The MORBID code is useful mainly for standard rigid molecules. It takes an advantage of Morse oscillator basis functions, for which the matrix elements of pure stretching motion are known analytically. However, the bending basis functions are evaluated in the framework of a numerical integration technique, which can be a time-consuming step. Modern fully variational approaches use a finite basis representation of the vibrational space: as the TROVE implementation in principle allows to perform variational calculations for general polyatomic molecules of arbitrary structure. However in that approach, the kinetic energy operator is represented only approximately as a power expansion in terms of internal coordinates. That approximation produces adequately accurate energy levels only rather low in energy, where the wavefunction has a limited spread around the molecular equilibrium position, where the power expansion is accurate.

The present work introduces a virtually exact variational method, which joins the main advantages of (i) simple algebraic forms of matrix elements, (ii) completeness of the basis set, and (iii) sparseness of the resulting Hamiltonian

---

\*Electronic address: Tereza.Sedivcova@gmail.com

matrix. In concrete, we describe the stretching modes with a formalism based on the Morse oscillator [9], with some similarity to the algebraic approaches of Ref. [10]. The main advantage of an potential expansion in terms of Morse coordinates is that one can use a quantum-mechanical basis on which the matrix representation of the Hamiltonian operator is sparse and can be computed analytically using algebraic techniques based on generalized step operators. For the bending mode we choose a cosine-power expansion of the potential and a quantum mechanical basis of spherical-harmonic functions. We then formulate and solve numerically the multi-dimensional problem of the vibrations of a polyatomic molecule in a product space of the different degrees of freedom. The sparse quality of the individual matrices representing the one-dimensional vibrations and the interaction terms carries forward to the global matrix representation of the total Hamiltonian on the product Hilbert space. The eigenvalues and eigenvectors of the resulting sparse matrix can then be obtained numerically quite efficiently by modern exact diagonalization tools. In principle, this method can be applied to molecules composed by any number of atoms, even though in practice the size of the product Hilbert space grows exponentially in the number of dimensions, which makes this method, like all virtually exact methods rather unpractical for molecules with 6 or more atoms. In this study we focus on triatomics, but we construct the theory in terms of basic building blocks usable for successive extensions to the multi-dimensional potential surfaces of polyatomic molecules, which will be the subject of future investigation.

The present approach bears some resemblance to Lie algebraic methods based on a Heisenberg formulation of quantum chemistry (the second quantization of the Schrödinger equation). Several previous studies [10, 11, 12, 13] use an algebraic approach where the full Hamiltonian operator is expanded in powers of  $\mathcal{C}$ , a Casimir operator of a suitable Lie algebra, for example as follows:  $\hat{H} = E_0 + \sum_{i=2}^k A_i [\mathcal{C}(O(2))]^i$ . The trouble with that kind of expansion is that it maps to an explicit first-quantized Hamiltonian form involving an intricate mixed potential and kinetic contributions, including high powers of the momentum operator and unphysical products of the momentum and position operators. To avoid such unwanted properties we express separately the potential  $V$  and kinetic  $T$  energy operators. This can be done within a convenient scheme of ladder operators defined by means of a suitable factorization method [9, 14].

Section II sketches the model used, including the Hamiltonian, basis functions for stretching and bending modes, and formulas for the matrix elements. Section III reports and discusses the vibrational spectra of OCS, HCN, NO<sub>2</sub>, and H<sub>2</sub>O as obtained with the present method. Section IV discusses the approximations involved in the present method and its future extensions.

## II. THEORY

We perform all calculations in the bond-length-angle internal coordinates, as illustrated in Fig. 1. This is the most suitable choice of variables for the potential expansion involving Morse functions.  $R_1$  and  $R_2$  represent the bond lengths between the central atom and the two end atoms,  $\theta$  is the bending angle at the central atom. Given the masses  $m_1$  and  $m_2$  of the end atoms and  $m_3$  of the central atom, we define the two diatom reduced masses  $\mu_1 = m_1 m_3 / (m_1 + m_3)$ ,  $\mu_2 = m_2 m_3 / (m_2 + m_3)$ . The vibrational Hamiltonian, composed by a kinetic and a potential part, can be expressed in atomic units ( $\hbar = m_e = q_e = 1$ ) as follows:

$$H(R_1, R_2, \theta) = T(R_1, R_2, \theta) + V(R_1, R_2, \theta). \quad (1)$$

The standard expression for the pure vibrational kinetic energy operator in internal coordinates [15, 16] is

$$\begin{aligned} T(R_1, R_2, \theta) = & -\frac{1}{2\mu_1} \frac{\partial^2}{\partial R_1^2} - \frac{1}{2\mu_2} \frac{\partial^2}{\partial R_2^2} \\ & -\frac{1}{2} \left( \frac{1}{\mu_1 R_1^2} + \frac{1}{\mu_2 R_2^2} - \frac{2 \cos \theta}{m_3 R_1 R_2} \right) \left( \frac{\partial^2}{\partial \theta^2} + \cot \theta \frac{\partial}{\partial \theta} \right) \\ & -\frac{\sin \theta}{m_3 R_1 R_2} \frac{\partial}{\partial \theta} + \frac{\cos \theta}{m_3} \left( \frac{1}{R_1} \frac{\partial}{\partial R_2} + \frac{1}{R_2} \frac{\partial}{\partial R_1} \right) - \frac{\cos \theta}{m_3} \frac{\partial^2}{\partial R_1 \partial R_2} \\ & + \frac{\sin \theta}{m_3} \frac{\partial}{\partial \theta} \left( \frac{1}{R_1} \frac{\partial}{\partial R_2} + \frac{1}{R_2} \frac{\partial}{\partial R_1} \right) - \frac{\cos \theta}{m_3 R_1 R_2} \\ & + \frac{1}{8} \left( \frac{1}{\mu_1 R_1^2} + \frac{1}{\mu_2 R_2^2} + \frac{2}{m_3 R_1 R_2} \right) \frac{1}{\cos^2(\theta/2)} \Pi_z^2. \end{aligned} \quad (2)$$

This expression is singular at four boundary regions: at  $R_i \rightarrow 0$ , and at the bending extremes  $\theta = 0$  and  $\theta = \pi$ . While the former constitute no serious practical problem, since the vibrational motion avoids these regions due to the strongly repulsive nature of the potential energy function  $V$  there, the angular singular points are easily reached by

the motion: in particular  $\theta = \pi$  is the angular minimum energy direction in the case of linear molecules, and this may require explicit care to obtain a numerically stable algorithm. Specifically, the  $\Pi_z$  operator in the final row, defined in Ref. [16], accounts for the rotations of the molecule around an axis attached to it and coincident with the molecular axis when the molecules reaches its linear configuration  $\theta = 180^\circ$ : to our purpose  $\Pi_z$  can be replaced everywhere with its eigenvalue  $m$ . The final term  $\propto \Pi_z^2$  describes the kinetic-energy contribution of a rotational degree of freedom of bent molecules (and in this case we omit it), but it is needed to account for the fourth vibrational degree of freedom describing the  $m = \pm 1$  “ $\Pi$ ”,  $m = \pm 2$  “ $\Delta$ ”, etc.... axially-rotating vibrational excitations of those molecules such as OCS and HCN which are linear in their equilibrium geometry. For simplicity, in the main text we will stick mostly to  $m = 0$ , while the Appendix shall deal with the general algebra describing an arbitrary integer value of  $m$ .

We use the following parameterization of the potential energy surface:

$$V(R_1, R_2, \theta) = \sum_{k_1, k_2, k_3=0}^{k_1+k_2+k_3 \leq N_e} a_{k_1 k_2 k_3} v_1(R_1)^{k_1} v_2(R_2)^{k_2} u(\theta)^{k_3}. \quad (3)$$

This power expansion is realized in terms of Morse-related functions

$$v_i(R_i) = e^{-\alpha_i(R_i - R_{i \min})} - 1, \quad (4)$$

for the stretching degrees of freedom  $i = 1$  or  $2$ , and in terms of trigonometric expressions  $u(\theta) = [\cos \theta - \cos \theta_{\min}]$  for the bending degree of freedom. Similar parameterizations are employed e.g., by P. Jensen in the MORBID code [17], also D. Xie and coworkers use this Morse-cosine expansion for several molecules, with the parameters first fixed to fit an *ab-initio* PES, and later adjusted to reproduce spectroscopic experimental data [18, 19].

As customary, to compute a variational solution of the eigenproblem corresponding to  $H$ , we resort to the expansion of the eigenfunctions of  $H$  on a product basis:

$$\Psi_v(R_1, R_2, \theta) = \sum_{j_1, j_2, j_3} c_v^{j_1 j_2 j_3} \Phi_{j_1 j_2 j_3}(R_1, R_2, \theta), \quad (5)$$

where  $v$  is a complete set of vibrational quantum numbers characterizing an eigenstate of  $H$ ,  $c_v^{j_1 j_2 j_3}$  are yet-to-be-determined expansion coefficients, and

$$\Phi_{j_1 j_2 j_3}(R_1, R_2, \theta) = \phi_{j_1}(R_1) \phi_{j_2}(R_2) Y_{j_3}(\theta). \quad (6)$$

The 1-dimensional basis functions  $\phi_{j_i}(R_i)$  for the stretching modes were discussed in detail in Refs. [9, 14]. In particular, we use here the generalized quasi-number state basis [14, 20], defined as follows:

$$\phi_{j_i}(R_i) = \sqrt{\frac{\alpha_i j_i!}{\Gamma(2\sigma_i + j_i)}} y_i^{\sigma_i} e^{-\frac{y_i}{2}} L_{j_i}^{2\sigma_i-1}(y_i), \quad j_i = 0, 1, 2, \dots, \quad i = 1 \text{ or } 2, \quad (7)$$

with

$$y_i = y_i(R_i) = (2s_i + 1) e^{-\alpha_i(R_i - R_{i \min})}. \quad (8)$$

Here  $L_n^\rho$  are generalized Laguerre polynomials,  $\Gamma$  is the standard Gamma function generalization of the factorial [21] and  $s_i$  and  $\sigma_i$  are suitable positive parameters, whose value we discuss below.

For the angular variable we use the following basis derived from the spherical harmonics

$$Y_l(\theta) = \sqrt{2\pi} Y_{l0}(\theta, \varphi) = N_l P_l(\cos \theta), \quad \text{with } N_l = \left(l + \frac{1}{2}\right)^{1/2} \quad (9)$$

$[P_l(\cos \theta)]$  are standard Legendre polynomials  $P_l(z) \equiv \frac{d}{dz^l} (z^2 - 1)^l / (2^l l!)$ , which form a convenient orthonormal basis set over the range  $0 \leq \theta \leq \pi$ , in the measure  $d \cos \theta$ . This basis was used successfully by Carter and Handy [15]. In that work the authors evaluated the matrix-element integrals numerically by Gauss-Legendre quadrature, while here we use analytical expressions detailed below.

As the Hamiltonian is a sum of terms, its matrix elements are also expressed as a sum of individual terms, and each one of them is expressed as a product of operators acting on the  $R_1$ ,  $R_2$  and  $\theta$  variables. Accordingly, the matrix elements of  $H$  are computed as sums of products of terms, each of which refers to one oscillator individually. For example, the matrix elements of one of the kinetic contributions in Eq. (2) are evaluated as

$$\langle \Phi_{j_1 j_2 j_3} | -\frac{\cos \theta}{m_3 R_1 R_2} | \Phi_{j'_1 j'_2 j'_3} \rangle = -\frac{1}{m_3} \langle \phi_{j_1} | \frac{1}{R_1} | \phi_{j'_1} \rangle \langle \phi_{j_2} | \frac{1}{R_2} | \phi_{j'_2} \rangle \langle Y_{j_3} | \cos \theta | Y_{j'_3} \rangle. \quad (10)$$

Each of these 1-dimensional matrix elements is then evaluated using the algebraic methods described below.

### A. Stretching-coordinate matrix elements

As a first step, all  $R_i$ -dependent terms in the Hamiltonian of Eq. (1) must be expressed as functions of the Morse variable  $y_i(R_i)$  of Eq. (8). In other words, the  $v_i(R_i)^{k_i}$  potential terms in Eq. (3) and the  $R_i^{-1}$  and  $R_i^{-2}$  terms in the kinetic energy operator Eq. (2) must be expressed in terms of the corresponding  $y_i(R_i)$ . This is accomplished immediately for the potential terms [14], by choosing for each mode  $i$  the same value of  $\alpha_i$  in the potential expansion terms (4) and in the definition of  $y_i(R_i)$ , Eq. (8), so that  $v_i \equiv y_i/(2s_i + 1) - 1$ . The matrix elements of  $R_i^{-1}$  and  $R_i^{-2}$  on the basis of Eq. (7) could be computed exactly by numerical integration, but that procedure would be contrary to the general spirit of the present method and very inefficient, since that procedure would produce a non-sparse matrix. We prefer to fit the kinetic terms with a sum of powers of  $v_i$ :

$$R_i^{-p} \simeq \sum_j^{B_{pi}} b_{pij} v_i(R_i)^j, \quad p = 1, 2. \quad (11)$$

An example of the quality of such a fit is illustrated in Fig. 2. The fit targets a reasonably wide region around the equilibrium point  $R_{i \min}$ , where it is extremely accurate, but it deteriorates especially in the large- $R_i$  dissociation region. The fitting function could be forced to reach the same large- $R_i$  limit as  $R_i^{-2}$ , but then the fit would deviate much more in the most important region near the minimum. Accordingly, we prefer to accept this deviation near dissociation, which causes negligible numerical error to the final spectra. The fitted  $R_i$ -ranges and the best-fit coefficients  $b_{1ij}$  and  $b_{2ij}$  of  $R_i^{-1}$  and  $R_i^{-2}$  for OCS, HCN, NO<sub>2</sub> and H<sub>2</sub>O are reported in the Table A of the supporting information [22]. Root mean square (RMS) deviations ranging from 3 to 20 cm<sup>-1</sup> are obtained for the fits based on Eq. (11), of the type exemplified in Fig. 2. In practice these deviations affect the computed vibrational band origins at a completely negligible level.

The full details of the formalism to construct the analytical matrix elements of the functions  $v_i(R_i)$  of Eq. (4) are reported elsewhere [9, 23]. Here we just note that the idea underlying the algebraic approach is ultimately related to supersymmetry, which provides several analytical relations for a class of exactly-solvable problems, including the Schrödinger equation for the Morse potential. We only report the basic expression of the matrix elements of the exponential function and of the first derivative term:

$$\langle \phi_{ij} | e^{-\alpha_i(R_i - R_{i \min})} | \phi_{ij'} \rangle = \frac{-C_{ij'} \delta_{j,j'-1} + 2(\sigma_i + j') \delta_{j,j'} - C_{ij} \delta_{j,j'+1}}{2s_i + 1}, \quad (12)$$

$$\langle \phi_{ij} | \frac{\partial}{\partial R_i} | \phi_{ij'} \rangle = \frac{\alpha_i}{2} (C_{ij'} \delta_{j,j'-1} - C_{ij} \delta_{j,j'+1}), \quad (13)$$

where  $C_{ij} = \sqrt{j(j + 2\sigma_i - 1)}$ . Based on these expressions, all matrix elements of every stretching term in the potential expansion Eq. (3) and in the kinetic terms expressed as in Eq. (11) can be computed exactly. The matrix representation of  $v_i(R_i)^{k_i}$  is  $(2k_i + 1)$ -band diagonal.

The computation of the spectrum of one pure-stretching mode through the exact diagonalization of algebraic matrices can be made substantially more efficient by choosing a properly adapted quantum-mechanical basis, specifically tuned to the molecular potential [14]. A better convergence of the calculation of a single oscillator improves the convergence of the full 3-dimensional spectral calculation for the triatomic molecule. For example, for the first stretching oscillator we consider

$$H_1(R_1) = -\frac{1}{2\mu_1} \frac{\partial^2}{\partial R_1^2} + \sum_{k_1=0}^{N_c} a_{k_1 0 0} v_1(R_1)^{k_1}. \quad (14)$$

The shape of the basis wavefunctions (7) is tuned by four parameters  $R_{1 \min}$ ,  $\alpha_1$ ,  $s_1$  and  $\sigma_1$ . We fix  $R_{1 \min}$  to the relevant equilibrium bond length, and in order to preserve the matrix sparseness we set  $\alpha_1$  to the value used in the definition of  $v_1(R_1)$ . By tuning the remaining  $s_1$  and  $\sigma_1$  one has a sufficient basis flexibility to improve substantially the numerical convergence of the single-oscillator problem [14] Eq. (14). We optimize the parameters  $s_i$  and  $\sigma_i$  by the minimization of the sum of the  $N_b$  lowest bound-state eigenenergies of the dimer, as defined in equation (25) of Ref. [14]. We optimize the energies of  $N_b = 20$  stretching bound states, which cover and far exceed the spectral range of interest. To get sub-cm<sup>-1</sup> accuracy, a number of basis functions  $N_{d_i} \simeq 30$  in the one-oscillator basis are usually sufficient. The values of the final optimized parameters  $s_i$  and  $\sigma_i$  adopted in all calculations are collected in Table I. In fact, when  $N_{d_i}$  is large enough the spectral accuracy depends only weakly on the value of the basis parameters  $s_i$  and  $\sigma_i$ , so that the reported values are not particularly critical.



## B. Bending-angle matrix elements

On the spherical harmonics basis Eq. (9), it is straightforward to express the matrix elements of powers of the  $\cos\theta$  function. The bending-angle dependence of the potential energy surface is then conveniently fitted to powers of  $(\cos\theta - \cos\theta_{\min})$ . In this basis, the bending potential matrix is sparse and can be expressed analytically. To evaluate the matrix elements of powers of  $z = \cos\theta$ , we use the following relations [21]:

$$\langle Y_l | z | Y_j \rangle = \frac{l}{\sqrt{(2j+1)(2l+1)}} \delta_{l,j+1} + \frac{j}{\sqrt{(2j+1)(2l+1)}} \delta_{l,j-1}, \quad (15)$$

$$\begin{aligned} \langle Y_l | z^2 | Y_j \rangle &= \frac{2j^2 + 2j - 1}{(2j-1)(2j+3)} \delta_{l,j} \\ &+ \frac{l(j+1)}{(j+l+1)\sqrt{(2j+1)(2l+1)}} \delta_{l,j+2} + \frac{j(l+1)}{(j+l+1)\sqrt{(2j+1)(2l+1)}} \delta_{l,j-2}, \end{aligned} \quad (16)$$

and in general, recursively

$$\langle Y_l | z^{k_3} | Y_j \rangle = \frac{j+1}{\sqrt{(2j+1)(2j+3)}} \langle Y_l | z^{k_3-1} | Y_{j+1} \rangle + \frac{j}{\sqrt{(2j+1)(2j-1)}} \langle Y_l | z^{k_3-1} | Y_{j-1} \rangle. \quad (17)$$

Like for stretching matrix elements, the matrix representing  $u(\theta)^{k_3}$  is  $(2k_3 + 1)$ -band diagonal.

The derivation of the kinetic bending matrix elements is described in Appendix A. The final result is the following simple tridiagonal expression:

$$\begin{aligned} \langle Y_l | T_{\text{bend}} | Y_j \rangle &= \frac{1}{2} \left( \frac{1}{\mu_1 R_1^2} + \frac{1}{\mu_2 R_2^2} \right) j(j+1) \delta_{l,j} \\ &- \frac{1}{m_3 R_1 R_2} \frac{1}{\sqrt{(2l+1)(2j+1)}} (l^3 \delta_{l,j+1} + j^3 \delta_{l,j-1}). \end{aligned} \quad (18)$$

The basis functions Eq. (9) are independent of the shape of the bending potential, which means that, for bent molecules in particular, the number of basis functions required by a given degree of convergence could become unreasonably large. Unfortunately, there is no way of optimizing the individual functions to any given angular potential, as we do for the stretching functions. One way to overcome this problem is to replace the angular functions (9) with suitably optimized linear combinations thereof, for example, obtained as low-energy eigenstates of a purely bending 1-dimensional problem based on  $T_{\text{bend}}$  plus the  $a_{00k_3}$  part of the potential expansion (3), as was suggested e.g., in Ref. [15] and Ref.s therein. Such kind of approach can lead to significant basis size reduction, but also, unfortunately, to entirely nonzero angular matrix elements, eventually leading to a less sparse total matrix of  $H$ .

## III. RESULTS

We come to illustrate the application of the proposed algebraic method to the calculation of the vibrational spectra of real triatomic molecules. We target mainly the purely vibrational energy levels ( $J = 0$ ). As trial systems we select two linear molecules, OCS and HCN, and two bent ones,  $\text{NO}_2$  and  $\text{H}_2\text{O}$ . They are all well studied by experimental as well as theoretical techniques which provide accurate spectra to compare with. In particular, for OCS,  $\text{NO}_2$  and  $\text{H}_2\text{O}$  the literature offers realistic PESs parameterized in the form (3) suitable for our method [18, 19, 24]. Accordingly, we have taken the PES function parameters  $a_{k_1 k_2 k_3}$  for OCS,  $\text{NO}_2$  and  $\text{H}_2\text{O}$  exactly as in the referred publications [25]. For HCN, we use the potential surface provided by Ref. [26] to fit an expansion of the type (3). All these PESs are determined starting from *ab initio* points, but then the function parameters  $a_{k_1 k_2 k_3}$  are adjusted so that the deviation between the calculated vibrational levels and the observed spectra is minimized. In the energy region considered, these PESs are accurate enough to allow one to predict even highly excited vibrational levels with great precision.

The values of the Morse exponential parameters  $\alpha_i$  and equilibrium positions  $R_{i\min}$  are collected in Table II. We fit the algebraic potential parameters  $a_{k_1 k_2 k_3}$  for HCN to 737 points obtained using the PES function as given in Ref. [26], restricted to the HCN side of the HCN-HNC isomerization transition. The angular range is  $\theta = 180^\circ$  to  $90^\circ$ , the coordinate ranges are  $R_{\text{HC}}/a_0 = 1.4$  to  $4.4$  and  $R_{\text{CN}}/a_0 = 1.6$  to  $3.0$ , with energy up to  $45\,000\text{ cm}^{-1}$ . Table B in the supporting information [22] reports the resulting best fit parameters  $a_{k_1 k_2 k_3}$ , which produce a RMS deviation of  $29\text{ cm}^{-1}$ .

As the bending frequency is usually smaller than stretching, and as the bending basis (9) cannot be optimized to the problem at hand, it is generally necessary to include a larger number  $N_{d3}$  of bending basis states. The minimum size  $N_d = N_{d1} N_{d2} N_{d3}$  of the matrix for the total Hamiltonian (1) which needs to be diagonalized for a very accurate and reasonably stable spectrum is eventually very moderate, of order  $N_d \sim 10^4$ . The nonzero matrix elements of  $H$  are of the order of  $\sim \left[ \frac{2}{3} \max(N_c, B_{11}, B_{12}, B_{21}, B_{22}) + 1 \right]^3$  in each row of the global matrix. For  $B_{ki} = 5 \geq N_c$ , as in most calculation of the present work, this yields approximately 80 nonzero matrix elements per row, i.e. a very sparse matrix to store and diagonalize.

Once the full matrix is constructed and stored, it is diagonalized using the Jacobi-Davidson method provided by the PRIMME package [27, 28] for sparse matrices. Table III summarizes the quality of the computed spectra, in terms of root mean squared (RMS) deviations between the observed and calculated vibrational energy levels. These levels cover an energy range extending from the ground state up to several thousand wavenumbers, as indicated in Table III. The good agreement with experiment shown by the small RMS deviations indicates both the high quality of the considered PES parameterizations and the satisfactory accuracy of the employed method. The complete spectral levels obtained by means of the present approach and their detailed comparison to experimental data for OCS, HCN, NO<sub>2</sub> and H<sub>2</sub>O are collected in Tables C, D, E, F in the supporting information [22]. For OCS we compute and compare to experiment also numerous  $\Pi$  ( $m = \pm 1$ ) states.

For the molecules for which spectra were computed before based on the same PES (but with a different approach to the solution of the quantum-mechanical problem) we obtain an essentially equivalent accuracy of the spectra, as shown by the similar RMS deviations reported in Table III. Basically all discrepancies with experiment are to be attributed to the lack of accuracy of the adopted PES. Table D in the supporting information [22] collects also a few predicted energy levels of HCN in the 7000 to 12000 cm<sup>-1</sup> spectral range. These calculated values are also in good agreement with previous calculations by Mourik *et al.* Table F in the supporting information [22] reports also a few predicted levels for H<sub>2</sub>O.

The level assignments in terms of local vibrations is not always straightforward. The wave function of each vibrational state can be analyzed and it always results in a complicated admixture of excitations of all three local vibrational modes. For instance, the OCS vibrational excitation at  $E_v = 2937.2$  cm<sup>-1</sup> consists mainly (35%) of  $v = (140)$  plus 21%  $v = (060)$ , plus other minor components, which confirms the traditional assignment (140) reported in Table C. However, for example the largest local component,  $v = (080)$ , of the OCS vibrational excitation near 3990 cm<sup>-1</sup> is 26%, while the component on its standard local assignment  $v = (160)$  is smaller (18%).

#### IV. DISCUSSION AND CONCLUSIONS

In the present work, we demonstrate the possibility to compute the vibrational spectrum of an arbitrary triatomic molecule based on its PES and using algebraic techniques for the analytical determination of the matrix elements. The advantages of this method include simple formulas for the matrix elements, moderate total Hilbert space size, sparseness of the Hamiltonian matrix, all cooperating to a fast and efficient diagonalization. The generalization of this method to four-atomic and larger molecules is in principle straightforward, and in these higher-dimensional contexts the reduced basis size for each degree of freedom is even more crucial. These advantages make this method a very promising tool for the analysis of the vibrational levels of small molecules.

The input of the present approach includes only the atomic masses and a reasonably dense numerical sampling of the PES: this is in principle within reach of *ab-initio* electronic structure quantum chemical calculations. We did carry out a calculation of the spectrum of HCN based on the *ab-initio* PES generated by a large set of DFT-LDA (density functional theory in the local-density approximation) calculations. Due to the known drawbacks of the LDA, the resulting spectrum shows deviations from the experimental levels of a few hundred cm<sup>-1</sup>, but it proves the possibility to compute even highly excited vibrational molecular states entirely from first principles, with no parameters adjusted to the observed spectroscopical data. When highly accurate quantum chemical methods are applied to a relatively fine and extensive determination of the PES of a triatomic molecule, it will be possible to obtain much better predictive power for a calculation entirely free from any experimental input.

If the PES is known to a high degree of accuracy even in the energy region near and slightly above dissociation, the present method can take advantage of the possibility to extend the basis set beyond the number of bound states to describe reliably weakly-bound pre-dissociation states in the quasi continuum. In the future, the present algebraic approach could be extended to the study of resonances in the continuum, bound-to-free transitions in infrared absorption, Franck-Condon processes and in principle even atom-molecule and molecule-molecule collisions. Other perspective applications include the area of non-rigid molecules (van der Waals complexes, quasi-linear molecules) [11] and potentials with many minima such as those occurring in torsional oscillations [12]. Note finally that a reliable description of the quantum vibrational dynamics could allow us to exploit the manageable Hamiltonian structure produced by the present method to the study of intramolecular vibrational-energy redistribution.

## Acknowledgments

The authors wish to thank A. Bordoni for useful discussion, T. Mourik and J. Tennyson for kindly providing the computer procedure for generating the pointwise HCN potential from their analytical function [26], and the supercomputing centers Cineca (Italy) and Metacentrum (Czech Republic) for computer time allocation. This work was supported by the European Union through e-I3 ETSF project (INFRA-211956) and NoE Nanoquanta (NMP4-CT-2004-500198). H.Y.A. acknowledges financial support by the Italian Ministry of Foreign Affairs support and cooperation programme with the Iraqi scientific and university system, managed by the Landau Network and Centro Volta, Como, Italy.

**Supporting Information Available:** Document No. ... contains the best-fit parameters describing the PES of HCN according to Eq. (3). This document also reports the  $b_{pik}$  best-fit parameters of Eq. (11) for the  $R_i^{-p}$  functions. This document also lists detailed tables of the computed vibrational band origins compared to experimental data. For HCN and H<sub>2</sub>O, a comparison is also made with spectral data calculated using different approaches. This material is available free of charge via the Internet at <http://pubs.acs.org>.

## APPENDIX A: ANGULAR MATRIX ELEMENTS

The kinetic energy operator, Eq. (2), contains terms proportional to  $\cot \theta$  and to  $[\cos(\theta/2)]^{-2}$ , which are singular at the boundary points  $\theta = 0$  and  $\pi$ . In fact  $\theta = \pi$  is an especially important configuration for linear molecules, and it should then be described smoothly. Luckily, since the integration implied in the matrix elements is performed over the variable  $z = \cos \theta$ , this divergence is not a problem, and all relevant matrix elements can be computed analytically using several properties of the spherical harmonics. For brevity, we replace the  $\theta$ -independent kinetic coefficients with the shorthand

$$a_1 = -\frac{1}{2} \left( \frac{1}{\mu_1 R_1^2} + \frac{1}{\mu_2 R_2^2} \right) \quad (\text{A1})$$

$$a_2 = \frac{1}{m_3 R_1 R_2}, \quad (\text{A2})$$

and define the pure bending part of  $T$  as

$$T_{\text{bend}}(\theta) = (a_1 + a_2 \cos \theta) \left( \frac{\partial^2}{\partial \theta^2} + \cot \theta \frac{\partial}{\partial \theta} \right) - a_2 \left( \sin \theta \frac{\partial}{\partial \theta} + \cos \theta \right) + \frac{a_2 - a_1}{2} \frac{1}{1 + \cos \theta} \Pi_z^2. \quad (\text{A3})$$

In terms of  $z = \cos \theta$ ,  $\frac{\partial}{\partial \theta} \rightarrow -\sin \theta \frac{\partial}{\partial \cos \theta} = -(1-z^2)^{1/2} \frac{\partial}{\partial z}$ , and  $\frac{\partial^2}{\partial \theta^2} \rightarrow \sin^2 \theta \frac{\partial^2}{\partial \cos^2 \theta} - \cos \theta \frac{\partial}{\partial \cos \theta} = (1-z^2) \frac{\partial^2}{\partial z^2} - z \frac{\partial}{\partial z}$ , the angular kinetic energy is conveniently decomposed as

$$\begin{aligned} T_{\text{bend}}(z) = & a_1(1-z^2) \frac{\partial^2}{\partial z^2} \rightarrow T_1 \\ & + a_2 z(1-z^2) \frac{\partial^2}{\partial z^2} \rightarrow T_2 \\ & + a_1(-2z \frac{\partial}{\partial z}) \rightarrow T_3 \\ & + a_2(-2z^2 \frac{\partial}{\partial z}) \rightarrow T_4 \\ & + a_2(1-z^2) \frac{\partial}{\partial z} \rightarrow T_5 \\ & - a_2 z \rightarrow T_6 \\ & + \frac{a_2 - a_1}{2} \frac{1}{1+z} m^2 \rightarrow T_7. \end{aligned} \quad (\text{A4})$$

We derive the matrix elements of  $T_{\text{bend}}$  in the general case of arbitrary integer  $m$ . Because for the  $m \neq 0$  “ $\Pi$ ”, “ $\Delta$ ”, etc. vibrational excitations of linear molecules, the  $T_7$  term is singular at  $\theta = 180^\circ$ , all its matrix elements in the  $Y_{l0}$  basis diverge: for general  $m$  we need then to consider the natural extension of the basis of Eq. (9), namely the one provided by the  $Y_{lm}$  spherical harmonics:

$$Y_l^m(\theta) = \sqrt{2\pi} Y_{lm}(\theta, 0) = N_{lm} P_l^m(\cos \theta), \quad \text{with } N_{lm} = \left[ \frac{(2l+1)(l-|m|)!}{2(l+|m|)!} \right]^{1/2}, \quad (\text{A5})$$

for  $l \geq |m|$ . For compactness, in the following we write the matrix elements in terms of associated Legendre polynomials  $P_l^m(z) \equiv (-1)^{(|m|+m)/2} (1-z^2)^{|m|/2} dP_l(z)/dz^{|m|}$ , i.e. we omit the normalization factor  $N_{lm}$ , and we use the notation  $P_l^{m'} = \frac{d}{dz} P_l^m$ . In the derivation of the  $T_{\text{bend}}$  matrix elements, we make use of the following identities for the associated Legendre polynomials:

$$(j+1-|m|)P_{j+1}^m(z) = (2j+1)zP_j(z) - (j+|m|)P_{j-1}^m(z), \quad (\text{A6})$$

$$(1-z^2)P_j^{m'}(z) = -jzP_j^m(z) + (j+|m|)P_{j-1}^m(z), \quad (\text{A7})$$

$$(1-z^2)P_j^{m''}(z) = 2zP_j^{m'}(z) - \left[ j(j+1) - \frac{m^2}{1-z^2} \right] P_j^m(z). \quad (\text{A8})$$

As a direct consequence of Eq. (A6), Eq. (15) generalizes to

$$\langle Y_l^m | z | Y_j^m \rangle = \frac{N_{jm}}{N_{lm}} \left( \frac{l-|m|}{2j+1} \delta_{l,j+1} + \frac{j+|m|}{2j+1} \delta_{l,j-1} \right), \quad (\text{A9})$$

and the recursive relation (17) generalizes to

$$\langle Y_l^m | z^{k_3} | Y_j^m \rangle = \frac{N_{jm}}{2j+1} \left( \frac{j+1-|m|}{N_{j+1m}} \langle Y_l^m | z^{k_3-1} | Y_{j+1}^m \rangle + \frac{j+|m|}{N_{j-1m}} \langle Y_l^m | z^{k_3-1} | Y_{j-1}^m \rangle \right). \quad (\text{A10})$$

These relations are also useful for the calculation of the potential matrix elements.

The individual kinetic terms are then expressed as

$$\langle P_l^m | T_1 | P_j^m \rangle = a_1 \langle P_l^m | (1-z^2) | P_j^{m''} \rangle \quad (\text{A11})$$

$$= a_1 \langle P_l^m | 2z | P_j^{m'} \rangle - a_1 j(j+1) \langle P_l^m | P_j^m \rangle + a_1 m^2 \langle P_l^m | \frac{1}{1-z^2} | P_j^m \rangle$$

$$\langle P_l^m | T_2 | P_j^m \rangle = a_2 \langle P_l^m | z(1-z^2) | P_j^{m''} \rangle \quad (\text{A12})$$

$$= a_2 \langle P_l^m | 2z^2 | P_j^{m'} \rangle - a_2 j(j+1) \langle P_l^m | z | P_j^m \rangle + a_2 m^2 \langle P_l^m | \frac{z}{1-z^2} | P_j^m \rangle$$

$$\langle P_l^m | T_3 | P_j^m \rangle = -a_1 \langle P_l^m | 2z | P_j^{m'} \rangle \quad (\text{A13})$$

$$\langle P_l^m | T_4 | P_j^m \rangle = -a_2 \langle P_l^m | 2z^2 | P_j^{m'} \rangle \quad (\text{A14})$$

$$\langle P_l^m | T_5 | P_j^m \rangle = a_2 \langle P_l^m | (1-z^2) | P_j^{m'} \rangle = -a_2 j \langle P_l^m | z | P_j^m \rangle + a_2 (j+|m|) \langle P_l^m | P_{j-1}^m \rangle \quad (\text{A15})$$

$$\langle P_l^m | T_6 | P_j^m \rangle = -a_2 \langle P_l^m | z | P_j^{m'} \rangle \quad (\text{A16})$$

$$\langle P_l^m | T_7 | P_j^m \rangle = \frac{a_2 - a_1}{2} m^2 \langle P_l^m | \frac{1}{1+z} | P_j^m \rangle. \quad (\text{A17})$$

By collecting everything together and simplifying we obtain

$$\begin{aligned} \langle P_l^m | T_{\text{bend}} | P_j^m \rangle &= -a_1 j(j+1) \langle P_l^m | P_j^m \rangle - a_2 (j+1)^2 \langle P_l^m | z | P_j^m \rangle \\ &\quad + a_2 (j+|m|) \langle P_l^m | P_{j-1}^m \rangle + \frac{a_1 + a_2}{2} m^2 \langle P_l^m | \frac{1}{1-z} | P_j^m \rangle. \end{aligned} \quad (\text{A18})$$

Accordingly, the bending kinetic matrix elements in the normalized basis  $Y_l^m$  are

$$\begin{aligned} \langle Y_l^m | T_{\text{bend}} | Y_j^m \rangle &= -a_1 j(j+1) \delta_{lj} - a_2 (j+1)^2 \langle Y_l | z | Y_j \rangle \\ &\quad + a_2 (j+|m|) \frac{N_{jm}}{N_{j-1m}} \delta_{l,j-1} + \frac{a_1 + a_2}{2} m^2 \langle Y_l^m | \frac{1}{1-z} | Y_j^m \rangle \\ &= -a_1 j(j+1) \delta_{l,j} \\ &\quad - \frac{a_2}{\sqrt{(2j+1)(2l+1)}} \left[ l^2 \sqrt{l^2 - m^2} \delta_{l,j+1} + j^2 \sqrt{j^2 - m^2} \delta_{l,j-1} \right] \\ &\quad + \frac{a_1 + a_2}{2} m^2 \langle Y_l^m | \frac{1}{1-z} | Y_j^m \rangle, \end{aligned} \quad (\text{A19})$$

where we have inserted the matrix elements of  $z$  from Eq. (A9), and combined the two non-Hermitian terms proportional to  $a_2$  into a final explicitly Hermitian expression. The important special case  $m = 0$  is reported as Eq. (18) in the main text. The matrix element in the final term is

$$\langle Y_l^m | \frac{1}{1-z} | Y_j^m \rangle = N_{lm} N_{jm} l_{\text{max}} [l_{\text{max}} + 1] K_m(l_{\text{max}}), \quad \text{with } l_{\text{max}} = \max(l, j), \quad (\text{A20})$$

and with

$$\begin{aligned} K_{\pm 1}(l) &= 1 \\ K_{\pm 2}(l) &= \frac{1}{2}(l^2 + l - 2) \\ K_{\pm 3}(l) &= \frac{1}{3}(l^4 + 2l^3 - 7l^2 - 8l + 12). \end{aligned}$$

Unfortunately the last term in Eq. (A19), the one proportional to  $m^2$  and originated by  $T_7$  plus parts of  $T_1$  and  $T_2$ , produces a matrix which, according to Eq. (A20), is not sparse on this basis. This leads to significant numerical overhead in the calculation of the  $m \neq 0$  states, with respect to the  $m = 0$  ones.

- 
- [1] Ulenikov, O.; Bekhtereva, E. S.; V., O.; Chudinova, T. D.; Jerzembeck, W.; Burger, H. *J. Mol. Spectrosc.* **2008**, *251*, 114.
- [2] Urban, S.; Herlemont, F.; Khelkhal, M.; Fichoux, H.; Legrand, J. *J. Mol. Spectrosc.* **2000**, *200*, 280.
- [3] Voitsekhovskaya, O. K.; Cherepanov, V. N.; Kotov, A. A. *Spectrochim. Acta A* **2004**, *60*, 1133.
- [4] Tennyson, J.; Miller, S.; Lesueur, C. R. *Comp. Phys. Com.* **1993**, *75*, 339.
- [5] Tennyson, J.; Kostin, M. A.; Barletta, P.; Harris, G. J.; Polyansky, O. L.; Ramanlal, J.; Zobov, N. F. *Comp. Phys. Commun.* **2004**, *163*, 85.
- [6] Jensen, P. *Comp. Phys. Rep.* **1983**, *1*, 1.
- [7] Yurchenko, S. N.; Thiel, W.; Jensen, P. *J. Mol. Spectrosc.* **2007**, *245*, 126.
- [8] Shirin, S. V.; Zobov, N. F.; Ovsyannikov, R. I.; Polyansky, O. L.; Tennyson, J. *J. Chem. Phys.* **2008**, *128*, 224306.
- [9] Bordoni, A.; Manini, N. *J. Quant. Chem.* **2007**, *107*, 782.
- [10] Iachello, F.; Levine, R. D. *Algebraic Theory of Molecules*; Oxford University Press, 1995.
- [11] Iachello, F.; Manini, N.; Oss, S. *J. Mol. Spectrosc.* **1992**, *156*, 190.
- [12] Iachello, F.; Oss, S. *Eur. Phys. J. D* **2002**, *19*, 307.
- [13] Iachello, F.; Perez-Bernal, F.; Vaccaro, P. H. *Chem. Phys. Lett.* **2003**, *375*, 309.
- [14] Bordoni, A.; Manini, N. *J. Phys. Chem. A* **2007**, *111*, 12564.
- [15] Carter, S.; Handy, N. C. *Mol. Phys.* **1982**, *47*, 1445.
- [16] Carter, S.; Handy, N. C. *Comp. Phys. Rep.* **1986**, *5*, 115.
- [17] Jensen, P. *J. Mol. Spectrosc.* **1988**, *128*, 478.
- [18] Xie, D. Q.; Lu, Y. H.; Xu, D. G. *Chem. Phys.* **2001**, *270*, 415.
- [19] Xie, D. Q.; Yan, G. *Chem. Phys. Lett.* **1996**, *248*, 409.
- [20] Molnar, B.; Foldi, P.; Benedict, M. G.; Bartha, F. *Europhys. Lett.* **2003**, *61*, 445.
- [21] Arfken, G. *Mathematical Methods for Physicists*; Academic Press, Orlando FL, 1985.
- [22] See Supporting Information, document No. ... for the best-fit parameters describing the PES of HCN according to Eq. (3). This document also reports the  $b_{pik}$  best-fit parameters for the  $R_i^{-p}$  functions. This document also lists detailed tables of the computed vibrational band origins compared to experimental data. For HCN and H<sub>2</sub>O, a comparison is also made with spectral data calculated using different approaches. This document can be accessed freely via a direct link from the present online article.
- [23] Lemus, R.; Arias, J. M.; Gomez-Camacho, J. *J. Phys. A* **2004**, *37*, 1805.
- [24] Xie, D. Q.; Yan, G. *Mol. Phys.* **1996**, *88*, 1349.
- [25] Attention must be paid to the signs before the potential terms. In the present work we use  $v(R) = \exp[-\alpha(R - R_{\min})] - 1$  whereas Xie *et al.*[18, 19, 24] use the quantity  $y(R) = 1 - \exp[-\alpha(R - R_{\min})]$  in a similar context. Also, some confusion arises for the bending terms of bent molecules. In Refs. [19, 24], it is claimed that calculations are based on the function  $Y_3(\theta) = \cos \theta_{\min} - \cos \theta$ , while in fact the PES data of those papers are consistent with a  $Y_3$  function coincident with our  $u(\theta) = \cos \theta - \cos \theta_{\min}$ .
- [26] van Mourik, T.; Harris, G. J.; Polyansky, O. L.; Tennyson, J.; Csaszar, A. G.; Knowles, P. J. *J. Chem. Phys.* **2001**, *115*, 3706.
- [27] Stathopoulos, A. *SIAM J. Sci. Comput.* **2007**, *29*, 481.
- [28] Stathopoulos, A.; McCombs, J. R. *SIAM J. Sci. Comput.* **2007**, *29*, 2162.

TABLE I: Optimized parameters  $s_i$  and  $\sigma_i$ , number of target bound states  $N_b$ , and size  $N_{d_i}$  of the quantum basis for each stretching oscillator of all molecules studied in the present work.

stretching dimer	optimized parameters		number of bound states	number of basis functions
	$s$	$\sigma$	$N_b$	$N_{d_i}$
OC	68.	40	20	30
CS	76.	52	20	30
HC	30.	0.20	20	40
CN	74.	46	20	30
OH	26.	0.01	20	30
NO	33.	5.04	20	30

TABLE II: The values of several relevant potential parameters for the molecules studied in the present work. The HCN parameters are obtained through a best fit to 737 points on the PES as computed in Ref. [26].

system	$R_{1\min}$ [ $a_0$ ]	$R_{2\min}$ [ $a_0$ ]	$\theta_{\min}$ [degree]	$\alpha_1$ [ $a_0^{-1}$ ]	$\alpha_2$ [ $a_0^{-1}$ ]	Reference
OCS	2.1849 (OC)	2.9506 (CS)	180.0	1.2382	1.0318	[18]
HCN	2.0135 (HC)	2.1793 (CN)	180.0	0.9727	1.2290	[26]
NO <sub>2</sub>	2.2435	2.2435	133.767	1.6853	1.6853	[24]
H <sub>2</sub> O	1.8112	1.8112	104.440	1.1769	1.1769	[19]

TABLE III: Basis size for the individual oscillators  $N_{d_i}$ , total basis size  $N_d$ , and standard deviations of the computed spectra to the available experimental vibrational levels and to previous calculations of the same levels.

system	number of basis function				num. of energy levels	up to energy [ $\text{cm}^{-1}$ ]	RMS deviation	
	$N_{d1}$	$N_{d2}$	$N_{d3}$	$N_d$			obs.-cal [ $\text{cm}^{-1}$ ]	obs.-Ref. [ $\text{cm}^{-1}$ ]
OCS	30	30	50	$45 \times 10^3$	145	8057	0.31	0.26 [18]
HCN	40	30	50	$60 \times 10^3$	34	12389	14.	12. [26]
NO <sub>2</sub>	30	30	55	$49.5 \times 10^3$	143	8979	1.7	2.1 [24]
H <sub>2</sub> O	30	30	50	$45 \times 10^3$	69	21247	5.6	1.2 [19]

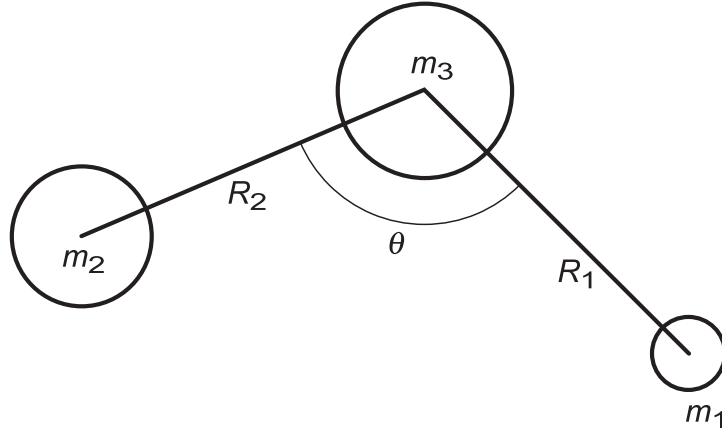


FIG. 1: The scheme of internal coordinates used in the present work.

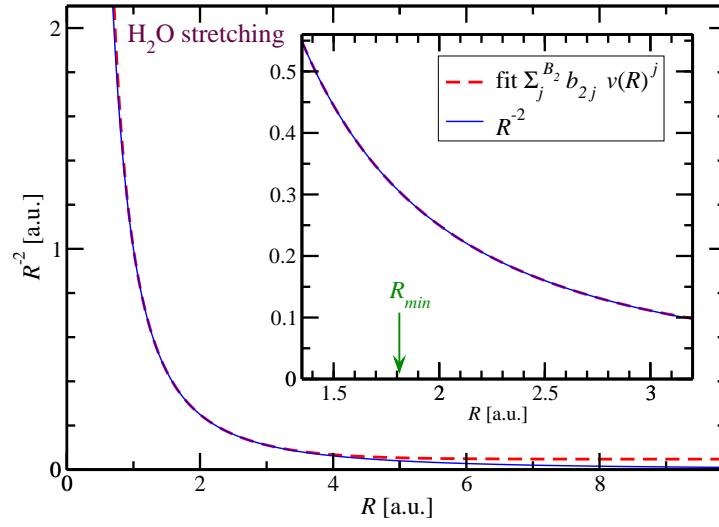


FIG. 2: Comparison between one of the  $R_i^{-2}$  function of Eq. (2), solid line, indicated simply as  $R^{-2}$ , and its fit in terms of Morse-related functions, Eq. (11), dashed line. In this calculation, relevant for the  $\text{H}_2\text{O}$  stretching coordinate  $R$ , the parameters  $\alpha \simeq 1.18 a_0^{-1}$ ,  $R_{\min} \simeq 1.81 a_0$ , and the expansion extends to order  $B_2 = 5$ . The coefficients  $b_{2j}$  are adjusted to obtain a best fit of equally spaced points in the  $1.35$  to  $3.2 a_0$  range of  $R$  highlighted in the inset.